Weather and Climate Extremes 36 (2022) 100455

Contents lists available at ScienceDirect

Weather and Climate Extremes

journal homepage: www.elsevier.com/locate/wace

Excess Heat Factor climatology, trends, and exposure across European Functional Urban Areas

Ana Oliveira [a,d], António Lopes [b,e,*], Amílcar Soares [c]

[a] IN+ Center for Innovation, Technology and Policy Research, Instituto Superior Técnico, Universidade de Lisboa, Portugal
[b] Centre of Geographical Studies, Institute of Geography and Spatial Planning, University of Lisbon, Portugal
[c] CERENA, Instituto Superior Técnico, Universidade de Lisboa, Portugal
[d] CoLAB +ATLANTIC, Portugal
[e] Associated Laboratory Terra, Portugal

ARTICLE INFO

Keywords:
Excess heat factor
Heatwaves
Europe
Functional urban areas
Heat exposure
Biogeographical regions

ABSTRACT

In Europe, regional climate change prospects indicate the urgency of adapting to extreme weather events. While increasing temperature trends have already been detected, in the last decades, the adoption of a European heatwave (HW) early-warning index is not yet consensual, partially due to the significant number of alternative algorithms, in some cases adjusted to the measurement of sector-specific impacts (as per the Expert Team on Climate Risk and Sector-specific Indices (ET-SCI)). In particular, the Excess Heat Factor (EHF) has been shown to accurately predict heat-related human health outcomes, in mid-latitude climates, provided that local summer exposure to excess heat is mostly driven by extreme air temperatures, with a lower contribution from relative humidity. Here, annual summaries of EHF-based HW detection were calculated for the European region, using daily maximum and minimum temperatures from the homogenised version of the E-OBS gridded dataset. Annual HW frequencies, duration, mean magnitude, maximum amplitude, and severity were subject to climatology and trend analysis across the European biogeographical regions, considering the 1961–1990 period as the baseline reference for anomaly detection in the more recent (1991–2018) decades. As HW-dependent morbidity/mortality affects mostly the elderly, an EHF-based HW Exposure Index was also calculated, by multiplying the recent probability of severe events per the number of people aged 65, or more, in the European Functional Urban Areas (FUAs). Results show that recent historical EHF-based patterns diverge across European Biogeographical regions, with a clear latitudinal gradient. Both the historical mean and recent trends point towards the greater exposure in the southern European Mediterranean region, driven by the significant increase of HW frequency, duration and maximum severity, especially in the last 3 decades; conversely, annual maximum EHF intensities (i.e., greatest deviations from the local 90th daily mean temperature) are mostly found in the northern and/or high altitude Boreal, Alpine and Continental regions, as a consequence of the latitudinal effect of local climatology on the HWM/HWA indices (this also translates into greater magnitudes of change, in this regions). Nonetheless, by simultaneously considering the probability of Severe HW occurrence in the last three decades, together with the log transformation of people aged 65 or more, results show that greater HW Exposure Indices affect FUAs across the whole Europe, irrespective of its regional climate, suggesting that more meaningful vulnerability assessments, early warning and adaptation measures should be prioritized accordingly.

1. Introduction

In Europe, regional climate change prospects point towards the urgency of adapting to exceptional weather events, such as floods, droughts or temperature extremes (Brunetti et al., 2004; European Environment Agency (EEA), 2005; Beniston et al., 2007; EEA, 2012; Kovats et al., 2014; Gudmundsson and Seneviratne, 2015; Spinoni et al., 2017). Particularly, increasing temperature trends - both seasonal/annual averages, and summer extremes - have already been detected, especially in the last two to three decades (Schär et al., 2004a; European Environment Agency (EEA), 2005; Beniston et al., 2007; EEA, 2012; Perkins et al., 2012; Kovats et al., 2014).

* Corresponding author. Centre of Geographical Studies, Institute of Geography and Spatial Planning, University of Lisbon, Portugal.
E-mail addresses: anappmoliveira@tecnico.ulisboa.pt (A. Oliveira), antonio.lopes@campus.ul.pt (A. Lopes), asoares@tecnico.ulisboa.pt (A. Soares).

https://doi.org/10.1016/j.wace.2022.100455
Received 1 July 2021; Received in revised form 8 March 2022; Accepted 22 April 2022
Available online 1 May 2022
2212-0947/© 2022 The Authors. Published by Elsevier B.V. This is an open access article under the CC BY-NC-ND license (http://creativecommons.org/licenses/by-nc-nd/4.0/).

While a consensual definition of extreme temperatures, or heatwave events (HW), has not been established (Perkins and Alexander, 2013; Perkins, 2015), different temperature-based indices have been used to investigate corresponding sectoral impacts – e.g. agriculture productivity (Harding et al., 2015), biological impacts (Cardoso et al., 2008), or energy needs (Mavrogianni et al., 2009) - allowing to extract appropriate information from daily weather observations, such as HW frequency, duration or intensity. Thorough assessments of such indices have been conducted by several authors (Perkins, 2015), and, despite the great diversity of definitions and statistical methods (Zhang et al., 2011), 27 climate indices developed by the World Climate Research Program (WCRP) and the sponsored Expert Team on Climate Change Detection and Indices (ET-SCI) provide a reference framework, along with the R-based ClimPACT tool to facilitate its calculation, ensuring quality control over the input data (Alexander et al., 2013; L and N., 2015; Alexander and Herold, 2016).

In particular, the Excess Heat Factor (EHF) (Nairn et al., 2009), is a significant indicator of heat-related human health impacts, across mid-latitude climates, namely human mortality and morbidity (Langlois et al., 2013; Nairn and Fawcett, 2013, 2014; Scalley et al., 2015; Hatvani-Kovacs et al., 2016b; Jegasothy et al., 2017a; Nairn et al., 2018). The rationale supporting the EHF definition is to identify and quantify extreme temperatures as the three-day mean air temperature deviation from the long-term percentile-based climatology, in a given day of the year (DOY), multiplied by the past month acclimatization index (if > 1) (Nairn and Fawcett, 2013).

As a result, the EHF is a quadratic function of both the long-term and short-term air temperature anomalies, and its magnitude reflects the human acclimatization to the local climate. Although the EHF does not include humidity in its calculation, it uses daily mean temperature (TM) as the simple average between the daily maximum (TX) and minimum (TN) temperature values, which is implicitly affected by relative humidity changes; hence, according to the authors (Nairn and Fawcett, 2013), the EHF provides local public health stake-holders with a simpler but efficient method to estimate potential human excess heat exposure levels, compared to other bioclimatic indices, such as the Universal Thermal Climate Index (UTCI) (Zare et al., 2018), the Physiological Equivalent Temperature (PET) (Matzarakis et al., 1999) or Apparent Temperature (AT), which require additional weather variables in their calculations (this are usually used in thermal comfort studies).

Several studies have identified upward trends in HW-related indices, covering the whole or part of the European region, either using relative (Russo et al., 2015; Perkins-Kirkpatrick and Lewis, 2020) or absolute (Qiu and Yan, 2020) thresholds criteria. In some studies, links with temperature variability, atmospheric circulation or earth-system processes have also been addressed (e.g., Schär et al., 2004b; Jézéquel et al., 2018; Zhang et al., 2020). However, a Pan-European climatological EHF assessment is still lacking.

Regarding the HW exposure analysis, several studies have been conducted, recently, to determine the spatial incidence of heat-dependent impacts (Wolf and McGregor, 2013; Chambers, 2019; Smid et al., 2019). A great level of diversity exists regarding risk assessment terminologies, with different algorithms being proposed in the peer-reviewed literature (Bao et al., 2015; Ranke, 2016), from weighted average approaches (Tomlinson et al., 2011), dimension reduction strategies such as principal components or clustering analysis (Wolf and McGregor, 2013) or regression-based methods (Loughnan et al., 2012). Following a previous compilation of alternative definitions (Ranke, 2016), the formula proposed by the United Nations Disaster Relief Office (UNDRO, 1979) best summarises how a risk assessment index should be quantified. According to several authors, risk levels should be measured as a function of three components(Engle, 2011; Ranke, 2016; Thomas et al., 2019): (i) hazard exposure, comprising a given frequency, severity and items exposed, (ii) vulnerability, depicting the potential consequences of the exposure (e.g. mortality, economic losses), and (iii) preparedness, which is the system's ability to withstand those impacts. The author proposes that the first components should be combined through a multiplication approach: it ensures that, whenever the hazard's incidence does not overlap with items subject to its consequences (e.g., no population), the risk becomes null (Ranke, 2016).

In this study, annual summaries of EHF-based HW detection are analysed, to reveal regional patterns of HW frequency, duration, intensity and severity, as well as recent changes. In addition, given its track record on predicting human health outcomes, especially within the most sensitive social groups (e.g. elderly, children), an $HW_{EXPOSURE}$ Index is also proposed to prioritize HW adaptation in European main metropolitan regions. In these European Functional Urban Areas (FUAS) (European Union, 2016; Dijkstra et al., 2019), HW impacts are more likely to reach significant numbers, given the population concentration and the recent trends of an ageing population (United Nations, 2014; EUROSTAT, 2017).

2. Data and methods

2.1. Air temperature data

Input Daily Maximum (TX) and Minimum (TN) near-surface air temperature data corresponding to the extended summer season (from June to September) from the gridded Europe-wide ensemble dataset (E-OBS) - homogenised version '19.0eHOM', at $0.1^\circ \times 0.1^\circ$ spatial resolution - was retrieved from the EU-FP6 project UERRA (http://www.uerra.eu) and the Copernicus Climate Change Service, based on station observations data provided by the European Climate Assessment & Dataset (ECA&D project, available at https://www.ecad.eu) (Cornes et al., 2018).

The dataset includes the TN and TX 'best guess estimations' (mean value) of 100 ensemble members, covering a period from 1950 to 2018. It results from the interpolation of station-derived meteorological observations from the ECA&D initiative (Klein Tank et al., 2002; Klok and Klein Tank, 2009). While most stations' data have been previously quality-controlled by their providers, ECA&D follows additional procedures, including homogeneity tests and corrections (Royal Netherlands Meteorological Institute (KNMI), 2015a) and merges neighbouring series to provide a more complete blended series. Details on the homogeneity correction process for the gridded data itself have also been published (Squintu et al., 2020). Pre-processing of the original E-OBS TX and TN datasets was done with Climate Data Operators (CDO) (Schulzweida et al., 2009; Mueller and Schulzweida, 2011), to comply with ClimPACT instructions (Alexander et al., 2013).

2.2. Excess Heat Factor

The EHF calculation is the product of two excess heat sub-indices: (i) the Excess Heat Index Significance (EHIsig), which measures the 3-day difference to the 90th TM percentile of the reference period (here, 1961–1990); and (ii) the Excess Heat Index Acclimatization (EHIaccl) which measures the 3-day TM difference to the average TM of the preceding 30 days. While the former sub-index represents the excess heat as a long-term (climate-scale) anomaly, the later sub-index is intended to measure heat stress as a short-term anomaly, based on the principle that biological systems are less able to cope with a sudden rise in temperature (Nairn and Fawcett, 2013). The two sub-indices are calculated according to Equation (1) and Equation (2), and the EHF as per Equation (3), as follows (Nairn and Fawcett, 2013; Alexander and Herold, 2016):

$$EHI_{sig} = TM_{3-day} \cdot - \cdot TM_{90p} \quad \text{Eq.1}$$

$$EHI_{accl} = TM_{3-day} \cdot - \cdot TM_{30-day} \quad \text{Eq.2}$$

$$EHF = EHI_{sig} \times MAX(1, EHI_{acel}) \quad \text{Eq.3}$$

where TM3-day/TM30-day is average TM over 3/30 days, respectively (calculated as the average between TN and TX), and TM90p is the

90th percentile of TM for the correspondent calendar DOY. In the present study, each grid cell's 90th percentile threshold is calculated based on the 1961–1990 30-years baseline period (World Meteorological Organization, 2017), and the annual DOY curve is smoothed using a 15-days moving average (Alexander and Herold, 2016).

Whenever a positive EHF result is detected, its value is a quadratic measure of HW intensity, responding to both the long-term and short-term anomalies. The measurement unit is $^{\circ}C_L^2$, where the 'L' refers to the local nature of the threshold and EHF results, i.e., results are local-specific, and lower values are expected where the climate temperature range is lower (Nairn et al., 2018). The underlying rationale is the fact that similar quadratic responses to extreme HW have been documented regarding impacts on human health or energy (Ziser et al., 2005; Hatvani-Kovacs et al., 2016a; Jegasothy et al., 2017a; Nairn et al., 2018).

Following the framework of the ClimPACT tool (Perkins et al., 2012; Alexander et al., 2013), EHF results are gathered as annual HW time series, depicting five HW aspects to be used in the climatology and trends analysis: (i) annual Number of Heatwaves (HWN); (ii) annual Heatwave Days Frequency (HWF); (iii) annual Maximum Heatwave Duration (HWD); (iv) annual Mean Heatwave Magnitude (HWM); and (v) annual Maximum Heatwave Amplitude (HWA). It should be noted that the two HW intensity summaries (i.e., HWA and HWM) are inherently dependent upon the local temperature range, which varies in latitude. Hence, the HWA/HWM annual values and magnitude of change can only be compared meaningfully across different regions through local HW intensity normalization. To overcome this limitation, the EHF-based severity methodology ($EHF_{SEVERITY}$) has been included by the authors, to allow the identification of how extreme is a given HW day compared to local climatology (Nairn et al., 2018). The dimensionless $EHF_{SEVERITY}$ index is based on extreme value theory, corresponding to the normalization of each daily EHF intensity value by the 85th percentile (EHF85p) over a climatology period, as per Equation (4). Here, daily EHF intensities were normalized by the 85th percentile corresponding to the 1961–1990 period. To agree with the annual temporal resolution of the ClimpPACT outputs, daily $EHF_{SEVERITY}$ values were then summarised into an annual Maximum Heatwave Severity (HWS) time series.

$$EHF_{SEVERITY} = EHF \div EHF_{85p} \quad \text{Eq.4}$$

For the climatological analysis, mean annual values and standard deviation for reference 1961–1990 period were considered. Climatology and anomalies from 1991 to 2018 were also calculated, for comparison purposes. The HW trend significance was assessed through the non-parametric Mann-Kendall's test (statistical significance level computed at 5%) (Mann, 1945; Kendall, 1975; Sneyer, 1990), and the linear magnitude of change calculated per the Sen's method (Sen, 1968). The results are presented for the main continental European Biogeographical Regions (European Environment Agency (EEA), 2016).

2.3. HW exposure in Functional Urban Areas

To calculate HW exposure in European greater metropolitan areas, an existing methodology (Smid et al., 2019) was adapted to use the EHF index and the Functional Urban Areas (FUAS) inputs. In the original study (Smid et al., 2019), the authors propose an HW exposure level that results from the product between (i) the annual probability of HW occurrence (HW_{PROB}) per a given Heat Wave Magnitude Index-based (HWMId) threshold, and (ii) the population density of each capital city.

In this study, the authors' rationale of using normalization and multiplicative effect rational is maintained(Smid et al., 2019) (see). however, given the EHF specificity (health-related applications), several adaptations were required. Firstly, while in the original study the authors used three arbitrary HWMId threshold values for their probability assessment (selected per statistical distribution), here the $EHF_{SEVERITY}$ levels were considered. These have been supported by previous studies as appropriate proxies in identifying the thresholds of HW impacts (Nairn and Fawcett, 2013, 2014; Scalley et al., 2015; Hatvani-Kovacs et al., 2016b; Jegasothy et al., 2017a; Urban et al., 2017). According to the index authors (Nairn et al., 2018), HW events are considered Severe or Extreme when the $EHF_{SEVERITY}$ surpasses levels 1 or 3, respectively. Accordingly, to calculate HW_{PROB}, the number of years since 1991 (more recent climatological period) in which the annual HWS reaches the Severe level (i.e., maximum annual $EHF_{SEVERITY}$ equal or greater than 1) was divided by the time series size (i.e., 28 years) (see Equation (6)). Since strong upward trends and anomalies were detected in the more recent decades, only the last 28-years were considered in these statistics.

Secondly, while population density might reflect the number of people exposed, previous studies have pointed out how heat-related morbidity/mortality rates prevail upon the elderly (the most sensitive group) (Williams et al., 2012; Hatvani-Kovacs et al., 2016b; Jegasothy et al., 2017b). Hence, the number of people aged 65 is frequently introduced as contributing to the vulnerability assessment (e.g. Tomlinson et al., 2011; Wolf and McGregor, 2013). The $HW_{EXPOSURE}$ analysis focuses on the European Greater Metropolitan Areas, which corresponds to the Functional Urban Areas (FUAs) (Eurostat, 2016), and corresponding demographic statistics (for the 2008–2018 period) and vectorial geodata were retrieved from the EUROSTAT database (EUROSTAT, no date). The total 'number of people aged 65 or over' (POP_{65}) across the European FUAs shows an exponential statistical distribution – hence, a logarithmic transformation was applied (log_{10}-POP_{65}), followed by the normalization procedure, by dividing POP_{65} per the maximum $log_{10}POP_{65}$ across the FUAS ($nPOP_{65}$) (see Equation (7)).

$$HW_{EXPOSURE} = HW_{PROB} \times nPOP_{65} \; for \; HW_{SEVERITY} \geq 1 \quad \text{Eq.5}$$

$$HW_{PROB} = P(HW) = \frac{n(HW)}{n} \; for \; HWS \geq 1, \; in \; the \; 1991-2018 \; period \quad \text{Eq.6}$$

$$nPOP_{65} = \frac{log10POP_{65}}{\mathrm{MAX}(log10POP_{65})} \quad \text{Eq.7}$$

As both inputs correspond to normalized values, in a 0–1 scale, the exposure level translates also into a dimensionless (0–1) index (Equation (5)). The resulting $HW_{EXPOSURE}$ expresses, in the range 0–1, the level of exposure, where an $HW_{EXPOSURE}$ value of 1 means that both the maximum nHW_{PROB} and $nPOP_{65}$ are found in a given FUA.

3. Results

3.1. Excess Heat Factor climatology and trends

Figs. 1 and 2 illustrate the EHF-based climatology maps of 1961–1990 and 1991–2018, depicting the most significant HW aspects of the extended summer season (June–September): the number of events (HWN), number of days (HWF), maximum duration (HWD), mean magnitude (HWM), maximum amplitude (HWA) and maximum $EHF_{SEVERITY}$ (HWS). Recent anomalies are also shown as the percentage deviation between these two adjacent 30-years periods. Fig. 3 depicts the corresponding Sen's linear trend estimation with hashed regions highlighting the Mann-Kendall 95% significance level. The results can be interpreted as the magnitude of the average decadal rate of change, over the full 59-year period (long term), and time series plots for HWN and HWS are also shown per the European Biogeographical regions (Figs. 5 and 6).

Results show that an aggravation tendency of EHF-based HW events is common to the whole European region, with the greatest anomalies found in the frequency and maximum intensity/severity HW aspects (i.e., HWN, HWF, HWA and HWS in Figs. 1 and 2). The greatest HW frequencies (HW events or days) are found in Southern Europe, particularly in the Mediterranean bioregion, where the annual number of HW events has increased from an average of 2.4events/year in 1961–1990 to 4.5events/year in 1991–2018, at an average rate of 0.5vents/decade.

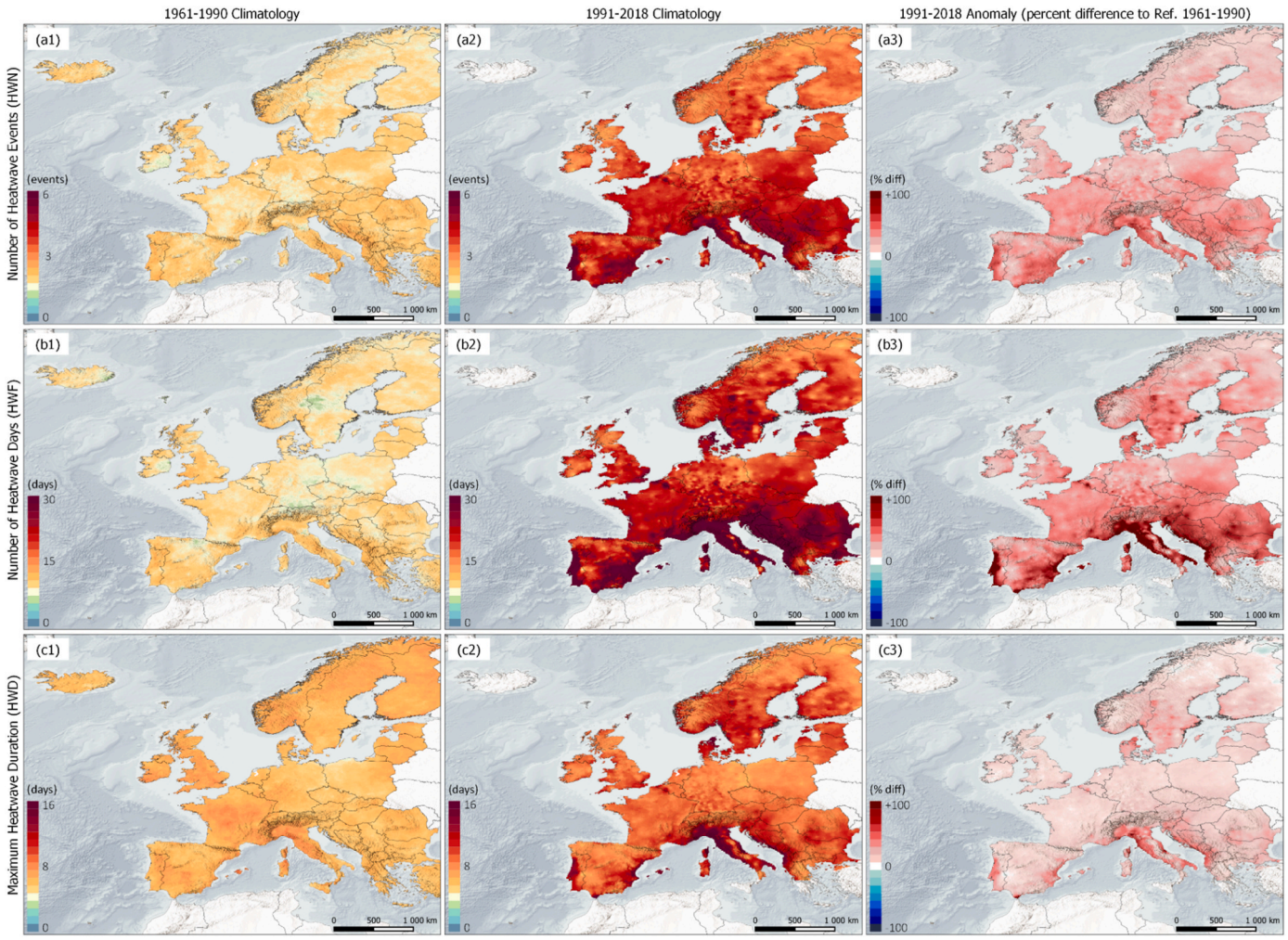

Fig. 1. Climatology (1961–1990 and 1991–2018) and anomaly (percentage difference) of EHF-based HW frequency and duration annual summaries: (a1-a3) number of HW events (HWN), (b1-b3) number of HW days (HWF); and (c1-c3) maximum duration of HW events (HWD). Due to missing data in the E-OBS dataset (in more recent years), some parts of south-eastern Europe (eg., southern Greece, Turkey) are omitted in the 1991–2018 climatology and anomaly analysis.

These numbers are even greater when the HWF is considered, with HW days increasing more than twofold in the more recent 1991–2018 period (on average, from 11.8 to 28.3 day/year). In particular, more than 30 EHF-based HW days (i.e., daily TM surpassing the 90th percentile of the 1961–1990 reference period) have been occurring per year in extended areas of the Iberian and Italian Peninsulas, and in Southeast Europe, since 1991. Accordingly, the greatest HWF upwards trends are also found in the Mediterranean, with HW frequencies increasing at a rate of 3.7 day/decade. Nonetheless, significant HWN/HWF increases are detected in every European biogeographical region, except in Northern Scandinavia. The same pattern is found regarding the HW duration aspect, HWD. On the other hand, the greatest climatological mean/maximum HW intensities (HWM/HWA) are found in the higher latitudes and altitudes, particularly in the highest mountain areas such as the Alps, Pyrenees or the Scandinavian Mountains. The trend analysis regarding the annual mean HW magnitude (HWM) is the only case of overall non-significant results. By contrast, the annual maximum HW amplitude (HWA) has been increasing significantly in almost all Europe, with maximum positive rates of change in the Pannonian region (2.0°C^2_L/decade), and throughout the Continental and Boreal Biogeographical regions (1.7 and 1.9 °C^2_L/decade, on average). Another relevant finding is that, in this Boreal region, variability has also increased, especially since 2000 – not only are annual summaries reaching new maximum values, but also, in some years, reaching or surpassing previous minimums.

However, it should be noted that these values are only suitable for local reference, as the EHF intensity is strongly dependent upon the local climatic range. Hence, a more meaningful inter-regional comparison can be drawn from the $EHF_{SEVERITY}$ annual summary, HWS, which shows that the greatest aggravation is found also in the Mediterranean, as well in the Pannonian regions, where an $EHF_{SEVERITY}$ level 1 (Severe HW event), has been reached, on average, every year since 1991. Nonetheless, a significant increase in the severity of HW events is also detected throughout most of the Continental and Atlantic regions, with cases of non-significant changes occurring in the British Isles and North of the Scandinavian Peninsula.

Both the HWF and HWS time series are presented in Figs. 4 and 5, where each panel shows the time series per Biogeographical region, and the boxplots depict the range of intra-region variability (quartiles and extremes).

While the climatologies show the spatial variation of the anomalies and the pixel-wise linear magnitude of change, these plots show also the increased variability that has been occurring in the last decades. In particular, Fig. 4 shows that while the number of HW days ranged from 0 to 20 before the '90s, this range has since shifted to 10–40 (Alpine, Continental regions) or 10–60 (Mediterranean, Continental, Boral and Pannonian). In Fig. 5, similar findings are shown, with Extreme HW (i.e., years when the annual maximum $EHF_{SEVERITY}$ surpasses level 3) becoming more frequent since 1990.

Finally, to provide a more practical synthesis, Table 1 presents the

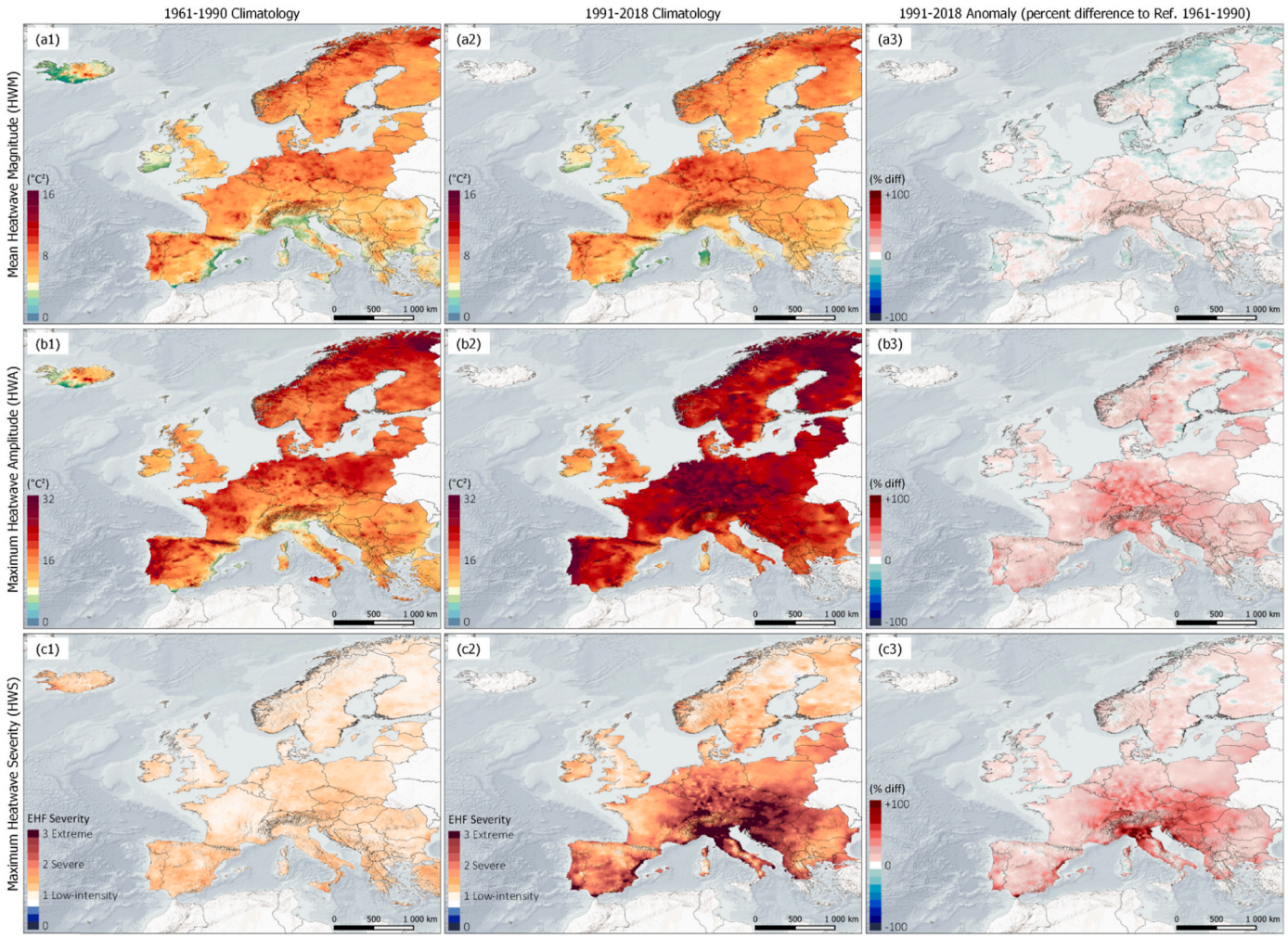

Fig. 2. Climatology (1961–1990 and 1991–2018) and anomaly (percentage difference) of EHF-based HW intensity and severity annual summaries: (a1-a3) mean HW magnitude (HWM), (b1-b3) maximum HW amplitude (HWA); and (c1-c3) maximum HW severity (HWS). Due to missing data in the E-OBS dataset (in more recent years), some parts of south-eastern Europe (eg., southern Greece, Turkey) are omitted in the 1991–2018 climatology and anomaly analysis.

aggregated statistics of the 1961–1990 and 1991–2018 periods, namely the spatial mean (standard deviation, s.d.) climatology and magnitude of change, per Biogeographical region – while this table highlights the average contrasts and variability between regions, it should be noted that the fixed nature of the Biogeographical delimitation may include non-homogenous HW patterns, which are better noticeable in the spatial patterns visible in Figs. 1–3.

3.2. Functional Urban Areas severe heatwaves exposure

The FUAs analysis provides further insights into which metropolitan regions should be prioritized in terms of the interaction between the probability of severe EHF-based HW events and the number of people exposed to them. Fig. 6 depicts the map of the FUAs location and their corresponding HW Exposure ($HW_{EXPOSURE}$) levels (from Equation (5)) overlaying the 85th percentile of the EHF intensity (1961–1990) which is the divisor in determining the severity threshold. The name of the FUAs where the $HW_{EXPOSURE}$ is equal to or greater than 0.4 are labelled on the map. In Fig. 7, the ranking of the 100 cities with greater $HW_{EXPOSURE}$ is shown, together with their probability of severe HW occurrence (HW_{PROB}) and the number of population aged 65 or more (POP_{65}). The results show that the position of the higher-ranked FUAs in the $HW_{EXPOSURE}$ index is mostly set by the population numbers, which was expected due to the exponential distribution (i.e., larger inter-FUAs contrasts) in this input, even if logarithmically transformed. Even though HW frequencies and severity are greater in the Mediterranean region (see the previous section), the probability of a severe HW (HW_{PROB}) has small variations amongst FUAs in the last 28 years, ranging from 70 to 100% in most cases. FUAs located in the Continental (41 cases) and Atlantic (36 cases) biogeographical regions are the most represented, due to the concentration of large cities in central European states, where both the numbers of the elderly population and Severe HW probabilities are above-average.

Hence, several Continental and Atlantic conurbations surpassing a 70% probability of Severe HW occurrence in the last 28 years appear in the first 20 places (e.g., Milano, HW_{PROB} = 90%, POP_{65} = 1 080; Ruhrgebiet, HW_{PROB} = 82%, POP_{65} = 1 100; Paris, HW_{PROB} = 75%, POP_{65} = 17470; Frankfurt, HW_{PROB} = 96%, POP_{65} = 500; Stuttgart, HW_{PROB} = 93%, POP_{65} = 530; or Berlin, HW_{PROB} = 77%, POP_{65} = 1 015). Nonetheless, cases such as London (POP_{65} = 1623, HW_{PROB} = 64%) are placed lower, compared to FUAs of equivalent elderly population size (e.g., Paris, HW_{PROB} = 75%, POP_{65} = 17470).

This order is intertwined with expected cases of greater $HW_{EXPOSURE}$ driven also by the greatest probabilities found in the Mediterranean region (in many cases, HW_{PROB} = 100%), such as Madrid (HW_{PROB} = 89%, POP_{65} = 1 061), Roma (HW_{PROB} = 86%, POP_{65} = 869), Barcelona (HW_{PROB} = 77%, POP_{65} = 877), Lisboa (HW_{PROB} = 93%, POP_{65} = 577), or Napoli (HW_{PROB} = 93%, POP_{65} = 536). These relative contrasts are useful in that they highlight how, in some cases, the number of vulnerable people is overcompensated by greater regional probabilities

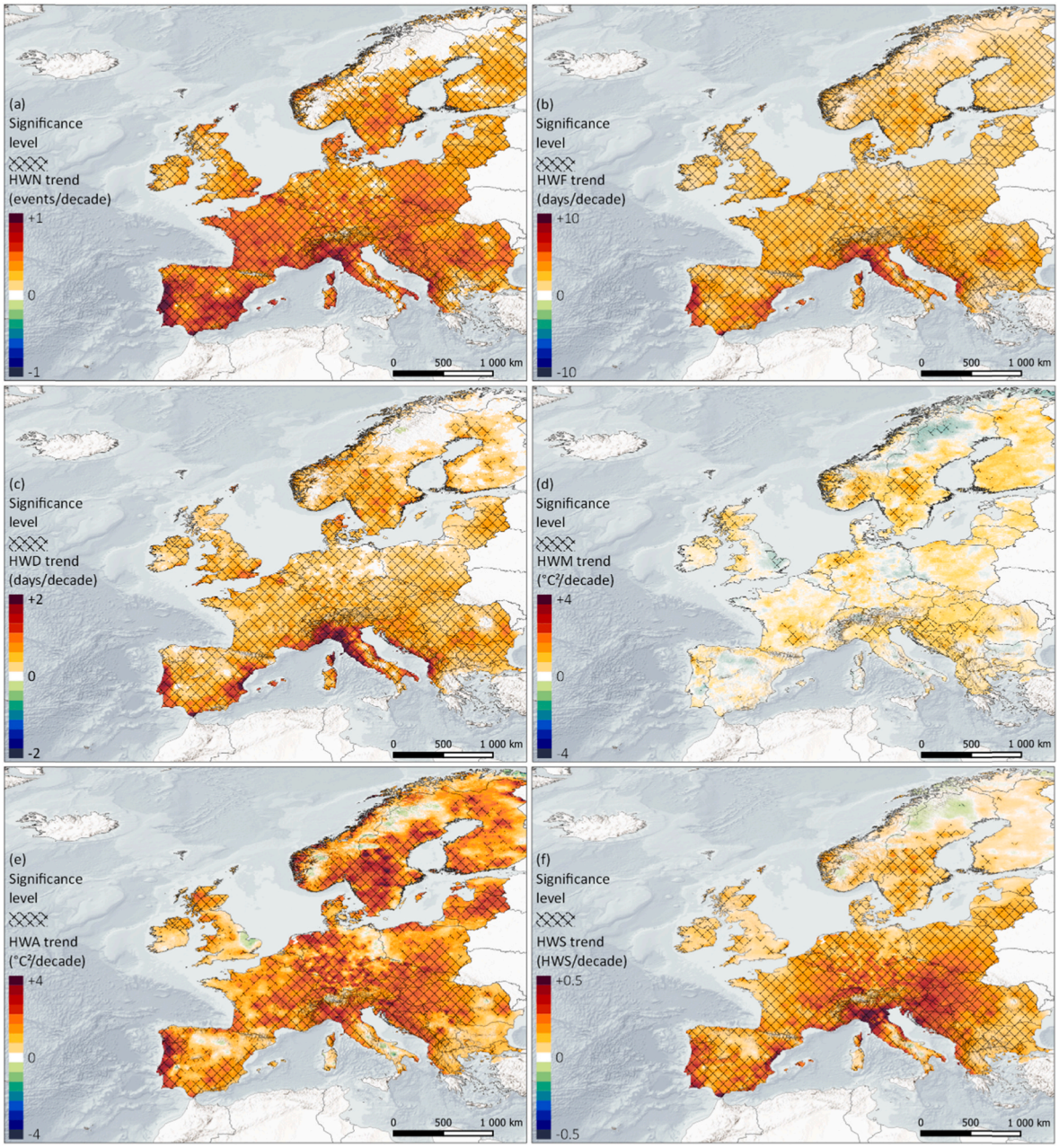

Fig. 3. Annual changes in HW events in Europe, from 1950 to 2018. Shaded gradient depicts the linear rate of change, as per Sen's slope estimation, and hashed pattern highlights Mann-Kendall significance at the 95% level. The trend analysis considers EHF-based annual summaries: (a) Number of HW events (HWN), (b) number of HW days (HWF); (c) maximum duration of HW events (HWD); (d) mean HW intensity (HWM), (e) maximum HW intensity (HWF); and (f) maximum HW severity (HWS). Due to missing data in the E-OBS dataset (in more recent years), some parts of south-eastern Europe (eg., southern Greece, Turkey) are omitted in the 1991–2018 climatology and anomaly analysis.

of being exposed to severe HW.

4. Discussion and conclusion

The implications of the present study can be framed within two scopes: (i) the climatology/trend findings, and (ii) the integration of these findings in public health actions.

Regarding the climatology and trend analysis, Several previous studies have been reporting a warming trend in the recent past and climate change prospects, over Europe (Giorgi et al., 2004; Giorgi, 2005; EEA, 2012; IPCC, 2014; Qiu and Yan, 2020), including the greater prevalence of extreme temperature summer events (Schär et al., 2004a; Russo et al., 2015; Zhang et al., 2020). European-level open data services, such as ECAD (Royal Netherlands Meteorological Institute (KNMI), 2015b), already provide several extreme temperature indices to the community, such as the number of Summer Days (SU) and Tropical Nights (TR), the Heatwave Duration Index (HWDI) or the percentage of warm days/nights (TX90p/TN90p). As with the Excess Heat Factor (EHF), these are also included in the sector-specific HW indices compiled by the ET-SCI and the corresponding ClimPACT tool but provide only HW frequency information. Examples of European studies are thus focused in such indices (Klein Tank and Können, 2003), in the analysis of the seasonal temperature frequency and anomalies distribution (Schär *et al.*, 2004), or the Heat-wave magnitude index daily (HWMId) (Russo et al., 2015). From these examples, only the HWMId provides a daily intensity measurement of the HW. Even if different

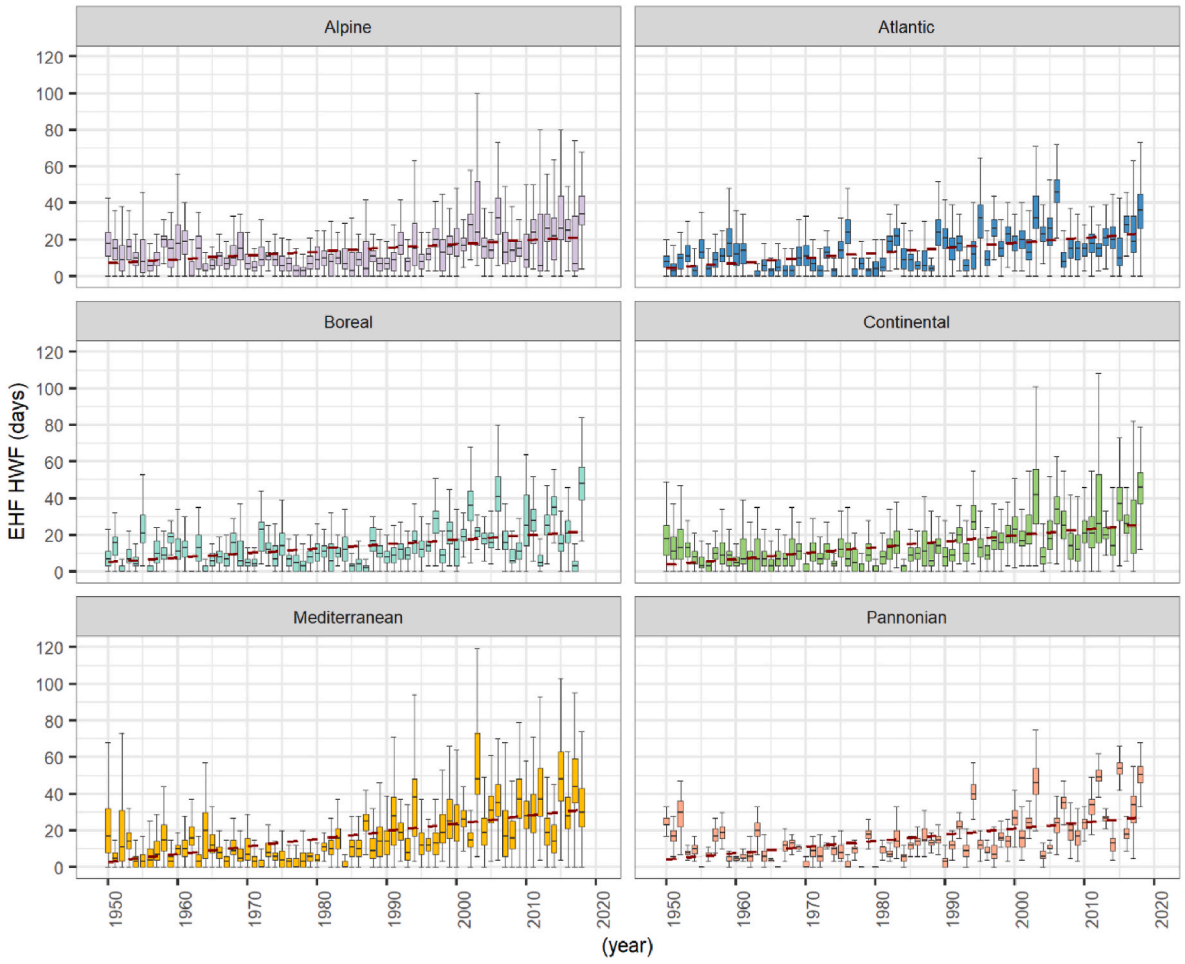

Fig. 4. Time series of annual Number of Heatwave Days (HWF), per European Biogeographical Regions. Boxplots represent the second and third quartiles within a region, per year, and error bars depict the upper/lower (90/10th) percentile limits.

index formulations prevent meaningful comparisons on the magnitude aspect of HW changes across studies, The present study agrees with previous regional findings as to the significant HW upward changes which can also be detected through the Excess Heat Factor (EHF), in Europe.

Accordingly, several parallels can be drawn. As with other cases of HW indices, (which methodology ranges from absolute to relative/percentile-based thresholds), HW occurrence is significantly increasing throughout Europe, particularly in the Mediterranean region where the greatest annual HW frequencies of events/days (HWN/HWF), duration (HWD) and maximum Severity (HWS) are detected in the more recent 1991–2018 period, compared to the baseline reference (1961–1990). This spatial Mediterranean aggravation detected in the EHF frequency and duration summaries (HWN, HWF and HWD) agrees with both the peer-reviewed literature (Kostopoulou and Jones, 2005; Beniston et al., 2007; Garcia-Herrera et al., 2010; Katavoutas and Founda, 2019), as well as international reports such as those from the European Environment Agency (EEA) or the Intergovernmental Panel on Climate Change (IPCC) (EEA, 2012; IPCC, 2014).

As per this study results, while HW frequencies are not surprisingly in agreement with other frequency-based metrics, the mean HW magnitude (HWM) has not changed significantly since 1950. Conversely, the annual strongest HW magnitude (HWA) and greatest HW severity (HWS) have significantly become more extreme, but as the EHF depicts local deviations from the historical climatology, the greatest HWA trends are noticeable in the higher latitudes and longitudes, where the climate is expected to be cooler. Such contrasts in the spatial patterns of the HW frequency versus HW amplitude suggest underlying shifts in the statistical distribution of the temperature anomalies themselves. Indeed, some authors have pointed out alternative schematics of potential changes in the probability of occurrence of temperature extremes (e.g., Perkins, 2015): (i) a shifted mean scheme, where the whole histogram is shifted upwards in the temperature axis (hence mean temperature augmenting and extreme cold extremes reducing); and (ii) an increased variability scheme where the histogram 'flattens' and both tails of the distribution reach values farther from the mean. In some regions, both changes may overlap. While the current analysis does not provide answers on these aspects, results suggest that, in the Mediterranean, the shifted distribution scenario might be the main HW increase culprit, whereas, in the Alpine, Continental and Boreal regions increased variability might also contribute – similar considerations can be found in other studies (Schär et al., 2004a; Fischer and Schär, 2010). Where statistical distribution shifts occur, it should be noted that the usage of climatological reference periods different from the one used in this study (1961–1990), particularly the most recent (and 'warmer') 30-years, would probably entail fewer events and/or smaller EHF maximums. The study is, however, limited to the WMO reference(World Meteorological Organization, 2017), which was particularly cooler; hence, the aspects resulting from this study can be interpreted as a 'worst-case scenario estimation', framed by the 1950–2018 available time series. Only full air temperature statistical distribution analysis, together with alternative thresholds comparison, could support or disprove these hypotheses of a climate shift and/or increased variability to support the adoption of a more recent baseline period to account for human

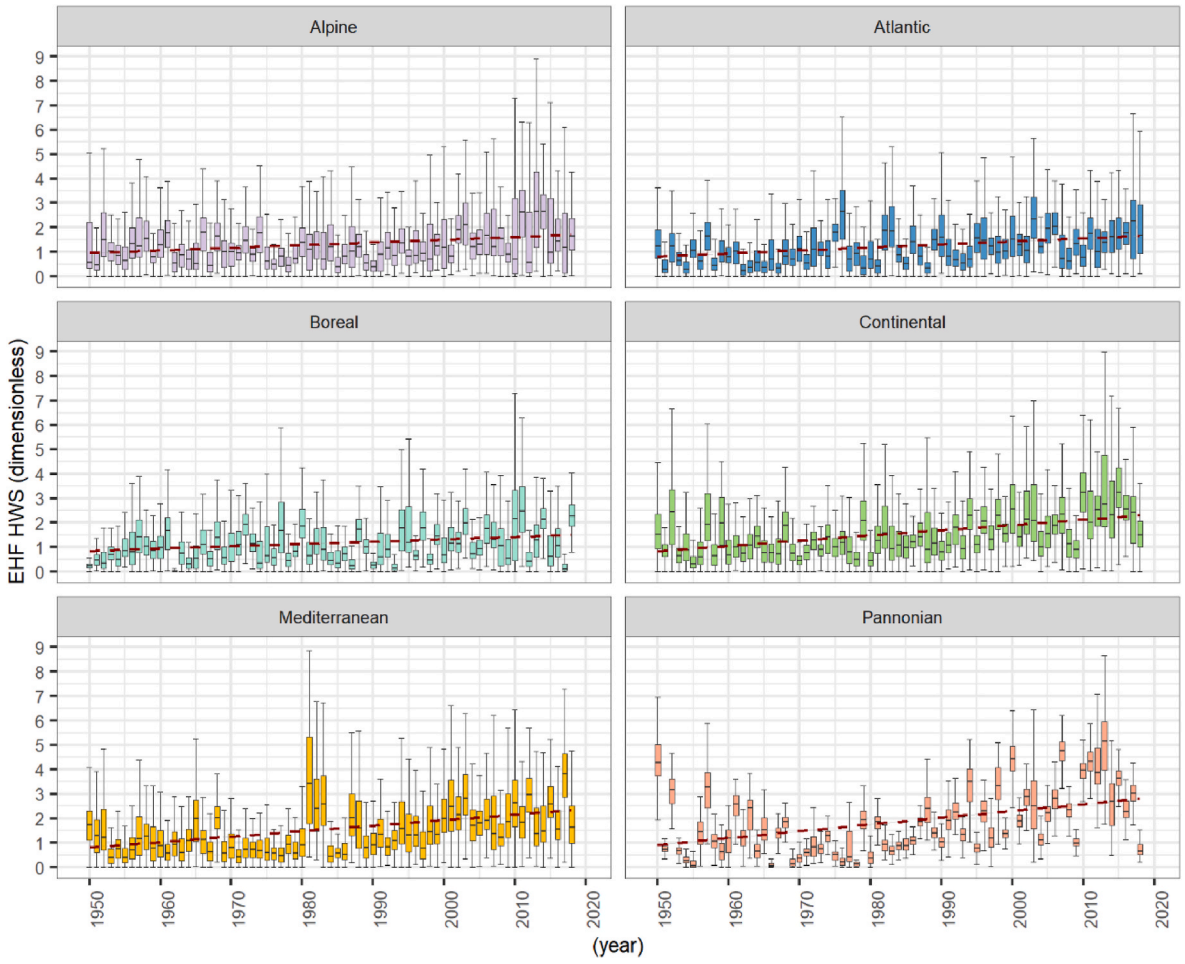

Fig. 5. Time series of annual Maximum Heatwave Severity (HWS), a dimensionless ratio between each year's HWA and the 85th percentile of the EHF intensity over the 1961–1990 reference period, per European Biogeographical Regions. Boxplots represent the second and third quartiles within a region, per year, and error bars depict the upper/lower (90/10th) percentile limits.

acclimatization capacity (which is in itself a topic being addressed in the literature (Bao et al., 2015; Hanna and Tait, 2015)).

On the other hand, the EHF distinguishes itself from other indices due to its ability to quantify the intensity and severity of each HW event (Nairn and Fawcett, 2013, 2014), which is a more significant predictor of acute human health response to extreme temperature exposure (Xu et al., 2016), compared to HW duration or frequency. As such, the outcome of this study is also linked with the implications of an increasing $EHF_{SEVERITY}$ in the scope of the European public health response. For example, while several studies have described historical changes in this index (Perkins et al., 2012; Perkins, 2015; Perkins-Kirkpatrick and Lewis, 2020), they have been focusing on other regions or the global scale, while EHF maps depicting the intra-European differences were still lacking – and this information on the spatial patterns of mensurable HW indices is required to pursue European-wide epidemiology studies on heat-dependent impacts, for informed regional decision making (Lass et al., 2012).

The EHF methodological specificity is tied to its ability to better predict human health outcomes, which respond non-linearly to temperature extremes, particularly in terms of human excess mortality and morbidity (Langlois et al., 2013; Nairn and Fawcett, 2013, 2014; Scalley et al., 2015; Hatvani-Kovacs et al., 2016b; Jegasothy et al., 2017a; Nairn et al., 2018). Recently, a public health study (Nairn et al., 2018) has tested the usage of the $EHF_{SEVERITY}$ to anticipate health impacts across the globe (Melbourne, Australia; London, United Kingdom; Chicago, United States of America; Paris, France; Moscow, Russia; Guangzhou, China), irrespective of the local climate. The authors have proved that a significant agreement exists between the maximum index values and local excess mortality or ambulance calls, from the time series of HW events in those case study cities. In addition, the authors show that the $EHF_{SEVERITY}$ anticipates by 1–2 days the date when the maximum health impacts are reached, a feature of importance for early warning systems (Lowe et al., 2011; McGregor et al., 2015; Vanderplanken et al., 2021) that is not always ensured by local-specific indices. For this reason, the $EHF_{SEVERITY}$ authors endorse its adoption at an international level (Nairn et al., 2018), following successful experiences in Australia (Nairn and Fawcett, 2014; Scalley et al., 2015; Hatvani-Kovacs et al., 2016c; Vanderplanken et al., 2021). Additional studies focusing on other locations have pointed to similar significant findings (Lin et al., 2012; Hatvani-Kovacs et al., 2016b; Urban et al., 2017; Tolika, 2019), which supports its usage for human heat exposure assessment.

In Europe, while many studies exist linking HW with excess mortality (Nogueira, 2005; Vandentorren et al., 2006; D'Ippoliti et al., 2010a, 2010b; Michelozzi et al., 2010; Sunyer, 2010; Laaidi et al., 2012; Morabito et al., 2012; Tobias et al., 2012; Heaviside et al., 2016; Arbuthnott and Hajat, 2017; Urban et al., 2017), these are mostly concerned with specific events and/or regions. There are, however, cases of EHF application describing promising results of its application in the European geographic domain (Nairn et al., 2018; Morais et al., 2020; Royé et al., 2020).

These preliminary findings support the usefulness of the $HW_{EXPOSURE}$ mapping analysis included in the present study, following the rationale

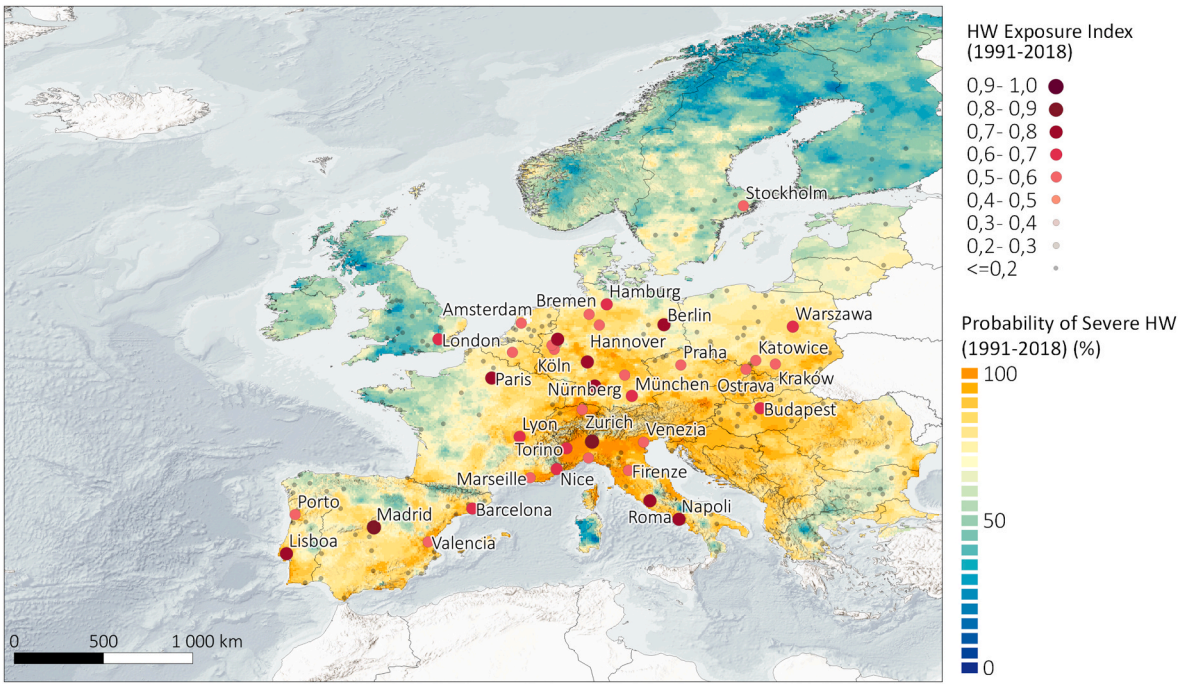

Fig. 6. Heatwave Exposure ($HW_{EXPOSURE}$) levels for the European Functional Urban Areas (FUAs) over Severe Heatwave Probability (HW_{PROB}) in the 1991–2018 period. Labelled FUAs have $HW_{EXPOSURE}$ levels equal or greater than 0.5 (0–1 normalized scale).

Table 1
EHF-based HW aspects per European biogeographical region: mean (s.d.) of annual summaries and magnitude of change, considering the extended summer (June–September) of two climatological periods (1961–1990 and 1991–2018).

Biogeographical regions	summary	HWN (events)	HWF (days)	HWD (days)	HWM ($°C_L^2$)	HWA ($°C_L^2$)	HWS (dimensionless)
Alpine	1961–1990	2.2 (±1.1)	10.7 (±6.6)	6.1 (±3.2)	7.6 (±5.3)	19.0 (±14.1)	1.2 (±0.8)
	1991–2018	3.6 (±1.9)	21.0 (±13.8)	8.6 (±4.3)	7.4 (±4.3)	24.8 (±16)	1.6 (±1.2)
	linear trend (decade^{-1})	0.2 (±0.2)	1.8 (±1.3)	0.3 (±0.3)	0.0 (±0.3)	1.2 (±0.8)	0.1 (±0.1)
Atlantic	1961–1990	2.4 (±1.4)	11.9 (±8.3)	6.4 (±3.3)	6.5 (±4.3)	17.3 (±12.6)	1.3 (±1)
	1991–2018	3.7 (±1.8)	21.0 (±12.1)	8.8 (±4.4)	6.6 (±3.9)	21.5 (±12.9)	1.5 (±1)
	linear trend (decade^{-1})	0.4 (±0.2)	2.5 (±0.7)	0.5 (±0.2)	0.1 (±0.2)	1.4 (±0.7)	0.1 (±0.1)
Boreal	1961–1990	2.2 (±1.2)	11.0 (±6.7)	6.3 (±3.3)	7.2 (±4.8)	18.7 (±12.7)	1.2 (±0.8)
	1991–2018	3.5 (±1.8)	21 (±13.2)	9.5 (±5.9)	6.9 (±4.5)	24.7 (±18)	1.4 (±1)
	linear trend (decade^{-1})	0.3 (±0.1)	2.0 (±0.7)	0.4 (±0.3)	0.2 (±0.2)	1.9 (±0.8)	0.1 (±0.1)
Continental	1961–1990	2.3 (±1.2)	10.6 (±6.7)	5.7 (±2.7)	6.8 (±4.2)	16.6 (±10.9)	1.3 (±0.8)
	1991–2018	4.1 (±2)	23.2 (±14.8)	8.8 (±4.7)	7.4 (±3.8)	24.4 (±13.2)	2.1 (±1.3)
	linear trend (decade^{-1})	0.5 (±0.1)	2.8 (±1.1)	0.5 (±0.3)	0.1 (±0.2)	1.7 (±0.7)	0.2 (±0.1)
Mediterranean	1961–1990	2.4 (±1.3)	11.8 (±8.1)	6.2 (±3.2)	5.4 (±4.2)	14.4 (±12.5)	1.4 (±1.2)
	1991–2018	4.5 (±2.2)	28.3 (±18.4)	10.2 (±5.9)	5.6 (±3.1)	20.2 (±12.5)	2.1 (±1.4)
	linear trend (decade^{-1})	0.5 (±0.2)	3.7 (±1.8)	0.8 (±0.5)	0.1 (±0.2)	1.3 (±0.8)	0.2 (±0.1)
Pannonian	1961–1990	2.4 (±1.2)	10.8 (±5.5)	5.6 (±2)	5.5 (±3.3)	14.1 (±9)	1.3 (±0.7)
	1991–2018	4.2 (±2.1)	24.2 (±14.8)	8.7 (±3.9)	6.8 (±3.1)	23.1 (±10.9)	2.6 (±1.4)
	linear trend (decade^{-1})	0.5 (±0.1)	2.8 (±0.6)	0.5 (±0.1)	0.3 (±0.1)	2.0 (±0.4)	0.3 (±0.1)

that human exposure is the product of the probability of a given harmful phenomenon multiplied by the number of susceptible individuals (Bao et al., 2015). Accordingly, the multiplicative methodology developed in a previous study (Smid et al., 2019) is here adapted for health-related impacts, to provide a ranking of which European urban areas are more exposed to Severe HW, in the last decades. Whether this algorithm (or any other) is the most suitable solution can only be validated by comparing its results with the human health consequences it aims to represent – a limitation that has not been addressed in this study due to the lack of access to consistent daily health (mortality and/or morbidity) data, at the European-level. Even in cases where such data is available (e.g., through national institutions), it is often difficult to access long or detailed enough time series for meaningful relations to be established (Nairn et al., 2018).

Limitations of its usage at the European level are mostly related to the lack of additional epidemiological studies comparing the EHF performance as an indicator for heat-dependant health impacts, across Europe. In addition, for the $HW_{EXPOSURE}$ index to evolve towards an $HW_{VULNERABILITY}$ indicator, as per several authors (Engle, 2011; Ranke, 2016; Thomas et al., 2019), additional confounders must be considered, such as the prevalence of vulnerable groups, the housing thermal performance or availability of indoor acclimatization solutions, the health care response capacity or the presence of aggravating/attenuating urban factors (e.g., urban heat island, the density of tree coverage). Hence, further advances in the use of these $HW_{EXPOSURE}$ indicators can be developed as soon as European-level health data becomes readily available.

Future developments of the present study should consider the several limitations mentioned, namely a simultaneous air temperature frequency analysis, reference periods comparison and performance

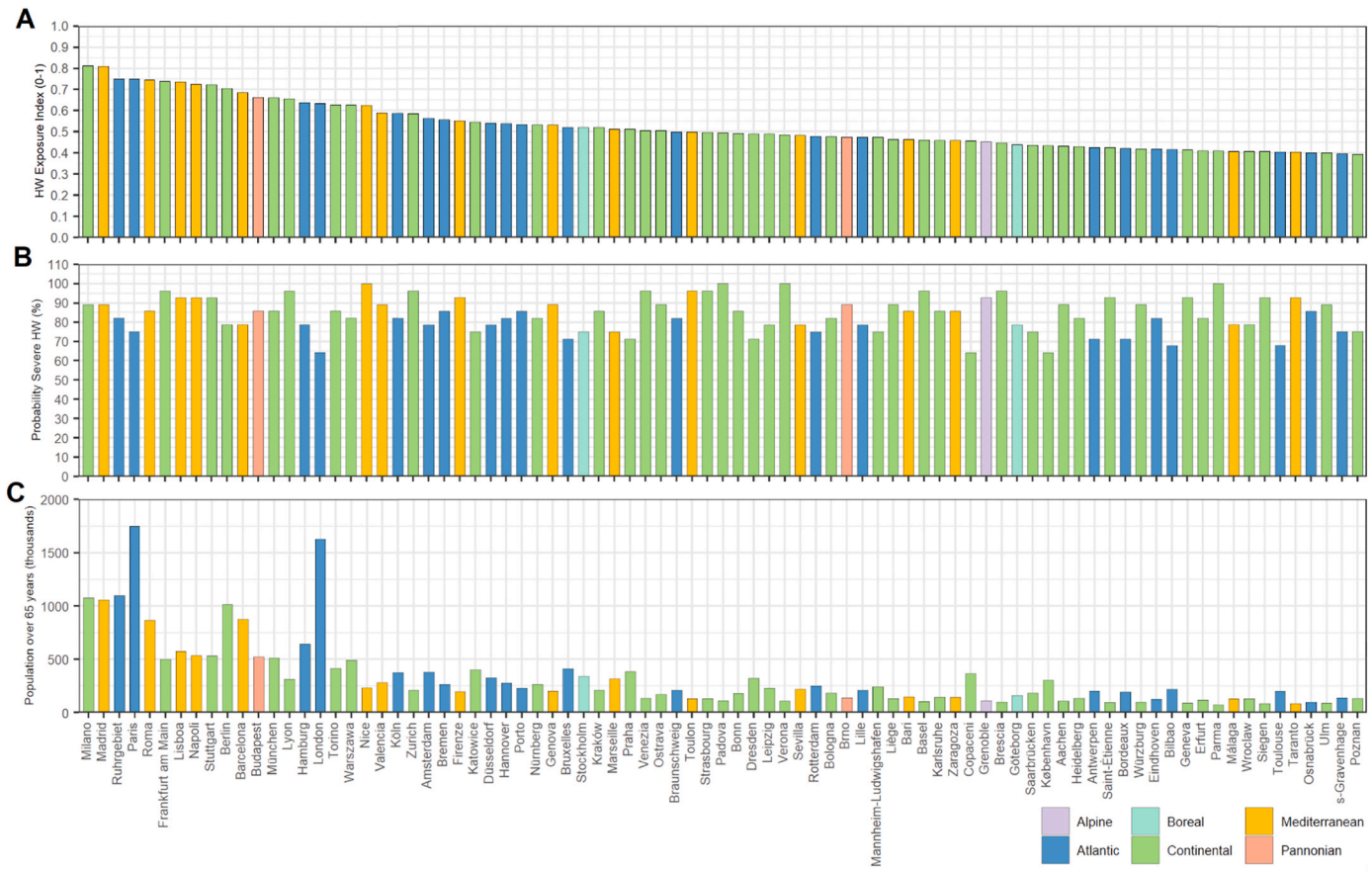

Fig. 7. Ranking results of the (a) Heatwave Exposure ($HW_{EXPOSURE}$) levels for the European Functional Urban Areas (FUAs), together with (b) probability of Severe HW and (c) Number of people aged 65 or over (2008–2018 period).

assessment on its relation with European heat-related health impacts, controlling for the above-mentioned confounders.

Funding

This research was funded by national funds through FCT – Fundação para a Ciência e a Tecnologia, I.P. [Ph.D. Grant NO. PD/BD/52304/2013].

This research was funded by FCT– Fundação para a Ciência e a Tecnologia, I.P. [CEG projects numbers: UIDB/00295/2020 and UIDP/00295/2020].

Author statement

Ana Oliveira: Conceptualization, Methodology, Formal analysis, Software, Visualization, Investigation, Writing- Original draft preparation. António Lopes: Resources, Supervision, Writing - Review & Editing. Amílcar Soares: Supervision, Writing - Review & Editing.

Declaration of competing interest

The authors declare that they have no known competing financial interests or personal relationships that could have appeared to influence the work reported in this paper.

Acknowledgements

We acknowledge the E-OBS dataset from the EU-FP6 project UERRA (https://www.uerra.eu) and the Copernicus Climate Change Service, and the data providers in the ECA&D project (https://www.ecad.eu).

The authors acknowledge the support received from the FCT – Fundação para a Ciência e a Tecnologia, I.P., through the Ph.D. Grant NO. PD/BD/52304/2013, as well as through the CEG projects numbers UIDB/00295/2020 and UIDP/00295/2020, and the Associated Laboratory Terra.

Appendix A. Supplementary data

Supplementary data to this article can be found online at https://doi.org/10.1016/j.wace.2022.100455.

References

Alexander, L., Herold, N., 2016. ClimPACT2 Indices and Software. University and of S. Wales, Sydney,Australia.

Alexander, L., Yang, H., Perkins, S., 2013. ClimPACT Indices and Software, Manual Prepared for the Workshop on Enhancing Climate Indices for Sector-specific Applications. CIIFEN Headquarters, Guayaquil, Ecuador.

Arbuthnott, K.G., Hajat, S., 2017. The health effects of hotter summers and heat waves in the population of the United Kingdom: a review of the evidence. Environ. Health 16 (1), 1–13. https://doi.org/10.1186/S12940-017-0322-5.

Bao, J., Li, X., Yu, C., 2015. The construction and validation of the heat vulnerability index, a review. Int. J. Environ. Res. Publ. Health 12, 7220–7234. https://doi.org/10.3390/ijerph120707220.

Beniston, M., et al., 2007. Future extreme events in European climate: an exploration of regional climate model projections. Climatic Change. https://doi.org/10.1007/s10584-006-9226-z [Preprint].

Brunetti, M., et al., 2004. Temperature, precipitation and extreme events during the last century in Italy. In: Global and Planetary Change. https://doi.org/10.1016/S0921-8181(03)00104-8.

Cardoso, P.G., Raffaelli, D., Pardal, M.A., 2008. The Impact of Extreme Weather Events on the Seagrass Zostera Noltii and Related Hydrobia ulvae Population. *Marine Pollution Bulletin*. https://doi.org/10.1016/j.marpolbul.2007.11.006.

Chambers, J., 2019. Global and cross-country analysis of exposure of vulnerable populations to heatwaves from 1980 to 2018. Climatic Change 163, 539–558. https://doi.org/10.1007/s10584-020-02884-2.

Cornes, R.C., et al., 2018. An ensemble version of the E-OBS temperature and precipitation data sets. J. Geophys. Res. Atmos. https://doi.org/10.1029/2017JD028200 [Preprint].
Dijkstra, L., Poelman, H., Veneri, P., 2019. The EU-OECD Definition of a Functional Urban Area. OECD Regional Development Working Papers. https://doi.org/10.1787/d58cb34d-en.
D'Ippoliti, D., et al., 2010a. The impact of heat waves on mortality in 9 European cities: results from the EuroHEAT project. Environ. Health: A Glob. Access Sci. Source 9 (1), 1–9. https://doi.org/10.1186/1476-069X-9-37/FIGURES/2.
D'Ippoliti, D., et al., 2010b. The Impact of Heat Waves on Mortality in 9 European Cities: Results from the EuroHEAT Project. *Environmental Health: A Global Access Science Source* [Preprint. https://doi.org/10.1186/1476-069X-9-37.
EEA, 2012. Climate Change, Impacts and Vulnerability in Europe 2012: an Indicator-Based Report. European Environment Agency. https://doi.org/10.2800/66071.
Engle, N.L., 2011. Adaptive capacity and its assessment. Global Environ. Change 21 (2). https://doi.org/10.1016/j.gloenvcha.2011.01.019.
European Environment Agency (EEA), 2005. Vulnerability and Adaptation to Climate Change in Europe. EEA Technical report No 7/2005. https://doi.org/10.1063/1.1647056.
European Environment Agency (EEA), 2016. Europe 2016 - the biogeographical regions. Available at: https://www.eea.europa.eu/data-and-maps/data/biogeographical-regions-europe-3. (Accessed 1 November 2020).
European Union, 2016. Urban Europe. Statistics on Cities, Towns and Suburbs: 2016 Edition, Urban Europe: Statistics on Cities, Towns and Suburbs. https://doi.org/10.2785/91120.
Eurostat, 2016. European Cities – the EU-OECD Functional Urban Area Definition - Statistics Explained. Eurostat web.
EUROSTAT, 2017. Eurostat Database," *Online Statistical Database* [Preprint]. https://doi.org/10.1109/TrustCom.2011.70.
EUROSTAT. Population on 1 January by age groups and sex - functional urban areas (urb_lpop1). Available at: https://ec.europa.eu/eurostat/web/cities/data/database. (Accessed 1 November 2020).
Fischer, E.M., Schär, C., 2010. Consistent geographical patterns of changes in high-impact European heatwaves. Nat. Geosci. 3 (6), 398. https://doi.org/10.1038/ngeo866.
Garcia-Herrera, R., et al., 2010. A Review of the European Summer Heat Wave of 2003. Critical Reviews in Environmental Science and Technology. https://doi.org/10.1080/10643380802238137 [Preprint].
Giorgi, F., 2005. Climate change prediction. Climatic Change. https://doi.org/10.1007/s10584-005-6857-4.
Giorgi, F., Bi, X., Pal, J.S., 2004. Mean, Interannual Variability and Trends in a Regional Climate Change Experiment over Europe. I. Present-Day Climate (1961-1990)," *Climate Dynamics*. https://doi.org/10.1007/s00382-004-0409-x [Preprint].
Gudmundsson, L., Seneviratne, S.I., 2015. European Drought Trends. *Proceedings of the International Association of Hydrological Sciences*. https://doi.org/10.5194/piahs-369-75-2015.
Hanna, E.G., Tait, P.W., 2015. Limitations to thermoregulation and acclimatization challenge human adaptation to global warming. Int. J. Environ. Res. Publ. Health 12 (7). https://doi.org/10.3390/ijerph120708034.
Harding, A.E., et al., 2015. Agro-meteorological Indices and Climate Model Uncertainty over the UK. *Climatic Change* [Preprint. https://doi.org/10.1007/s10584-014-1296-8.
Hatvani-Kovacs, G., et al., 2016a. Assessment of heatwave impacts. Procedia Eng. https://doi.org/10.1016/j.proeng.2016.10.039.
Hatvani-Kovacs, G., et al., 2016b. Can the Excess Heat Factor Indicate Heatwave-Related Morbidity? A Case Study in Adelaide. *EcoHealth*, South Australia. https://doi.org/10.1007/s10393-015-1085-5.
Hatvani-Kovacs, G., et al., 2016c. Can the excess heat factor indicate heatwave-related morbidity? A case study in Adelaide, South Australia. EcoHealth 13 (1), 100–110. https://doi.org/10.1007/S10393-015-1085-5.
Heaviside, C., Vardoulakis, S., Cai, X.M., 2016. Attribution of Mortality to the Urban Heat Island during Heatwaves in the West Midlands, UK. *Environmental Health: A Global Access Science Source* [Preprint. https://doi.org/10.1186/s12940-016-0100-9.
IPCC, 2014. Climate Change 2014: Impacts, Adaptation, and Vulnerability. Summary for Policymakers, Climate Change 2014: Impacts, Adaptation and Vulnerability - Contributions of the Working Group II to the Fifth Assessment Report. https://doi.org/10.1017/CBO9781107415416.005.
Jegasothy, E., et al., 2017a. Extreme climatic conditions and health service utilisation across rural and metropolitan New South Wales. Int. J. Biometeorol. https://doi.org/10.1007/s00484-017-1313-5.
Jegasothy, E., et al., 2017b. Extreme climatic conditions and health service utilisation across rural and metropolitan New South Wales. Int. J. Biometeorol. https://doi.org/10.1007/s00484-017-1313-5.
Jézéquel, A., Yiou, P., Radanovics, S., 2018. Role of circulation in European heatwaves using flow analogues. Clim. Dynam. https://doi.org/10.1007/s00382-017-3667-0 [Preprint].
Katavoutas, G., Founda, D., 2019. Intensification of thermal risk in Mediterranean climates: evidence from the comparison of rational and simple indices. Int. J. Biometeorol. https://doi.org/10.1007/s00484-019-01742-w.
Kendall, M., 1975. Multivariate Analysis. Charles Gr., London, UK.
Klein Tank, A.M.G., et al., 2002. Daily dataset of 20th-century surface air temperature and precipitation series for the European Climate Assessment. Int. J. Climatol. https://doi.org/10.1002/joc.773 [Preprint].
Klein Tank, A.M.G., Können, G.P., 2003. Trends in Indices of daily temperature and precipitation extremes in Europe, 1946-99. J. Climate. https://doi.org/10.1175/1520-0442(2003)016<3665:TIIODT>2.0.CO;2.
Klok, E.J., Klein Tank, A.M.G., 2009. Updated and extended European dataset of daily climate observations. Int. J. Climatol. https://doi.org/10.1002/joc.1779 [Preprint].
Kostopoulou, E., Jones, P.D., 2005. Assessment of Climate Extremes in the Eastern Mediterranean," *Meteorology And Atmospheric Physics*. https://doi.org/10.1007/s00703-005-0122-2.
Kovats, R.S., et al., 2014. Europe. In: Barros, V.R., et al. (Eds.), *Climate Change 2014: Impacts, Adaptation, and Vulnerability. Part B: Regional Aspects. Contribution Of Working Group II to the Fifth Assessment Report Of the Intergovernmental Panel On Climate Change*. Barros, V. Cambridge University Press, Cambridge, United Kingdom and New York, NY, USA, pp. 1267–1326.
L, A., N, H., 2015. ClimPACTv2: Indices and Software. Technical Report of the World Meteorological Organisation Commission for Climatology Expert Team on Sector-specific Climate Indices.
Laaidi, K., et al., 2012. The Impact of Heat Islands on Mortality in Paris during the August 2003 Heat Wave. *Environmental Health Perspectives* [Preprint. https://doi.org/10.1289/ehp.1103532.
Langlois, N., et al., 2013. Using the Excess Heat Factor (EHF) to predict the risk of heat related deaths. J. Forensic Legal Med. https://doi.org/10.1016/j.jflm.2012.12.005 [Preprint].
Lass, W., et al., 2012. Avoiding the avoidable: towards a European heat waves risk governance. Int. J. Disaster Risk Sci. 2 (1), 1–14. https://doi.org/10.1007/S13753-011-0001-Z.
Lin, S., et al., 2012. Excessive Heat and Respiratory Hospitalizations in New York State: Estimating Current and Future Public Health Burden Related to Climate Change. *Environmental Health Perspectives* [Preprint. https://doi.org/10.1289/ehp.1104728.
Loughnan, M., Nicholls, N., Tapper, N.J., 2012. Mapping heat health risks in urban areas. Int. J. Popul. Res. https://doi.org/10.1155/2012/518687.
Lowe, D., Ebi, K.L., Forsberg, B., 2011. Heatwave early warning systems and adaptation advice to reduce human health consequences of heatwaves. Int. J. Environ. Res. Publ. Health 8, 4623–4648. https://doi.org/10.3390/IJERPH8124623, 8(12), pp. 4623–4648.
Mann, H.B., 1945. Nonparametric Tests against Trend. Econometrica. https://doi.org/10.2307/1907187 [Preprint].
Matzarakis, A., Mayer, H., Iziomon, M.G., 1999. Applications of a universal thermal index: Physiological equivalent temperature. Int. J. Biometeorol. https://doi.org/10.1007/s004840050119 [Preprint].
Mavrogianni, A., et al., 2009. Space Heating Demand and Heatwave Vulnerability: London Domestic Stock. *Building Research and Information*. https://doi.org/10.1080/09613210903162597.
McGregor, G., et al., 2015. Heat Waves and Health: Guidance on Warning System Development. World Meteorological Organization [Preprint].
Michelozzi, P., et al., 2010. Surveillance of summer mortality and preparedness to reduce the health impact of heat waves in Italy. Int. J. Environ. Res. Publ. Health 7 (5). https://doi.org/10.3390/IJERPH7052256, 7.
Morabito, M., et al., 2012. Heat-related mortality in the Florentine area (Italy) before and after the exceptional 2003 heat wave in Europe: an improved public health response? Int. J. Biometeorol. https://doi.org/10.1007/s00484-011-0481-y, pp. 2256-2273.
Morais, L., Lopes, A., Nogueira, P., 2020. Which heatwave measure has higher predictive power to prevent health risks related to heat: EHF or GATO IV? – evidence from modelling Lisbon mortality data from 1980 to 2016. Weather Clim. Extrem. 30, 100287 https://doi.org/10.1016/J.WACE.2020.100287.
Mueller, R., Schulzweida, U., 2011. Climate Data Operators. Max-Planck-Institute for Meteorology [Preprint]. http://www.mpimet.mpg.de/~cdo.
Nairn, J., Fawcett, R., 2013. Defining heatwaves: heatwave defined as a heat-impact event servicing all community and business sectors in Australia, CAWCR technical report, 551.5250994.
Nairn, J., Fawcett, R., Ray, D., 2009. "Defining and predicting excessive heat events, a national system. In: Proceedings of the CAWCR Modelling. https://doi.org/10.1002/psc.518.
Nairn, J., Ostendorf, B., Bi, P., 2018. Performance of Excess Heat Factor Severity as a Global Heatwave Health Impact Index. *International Journal of Environmental Research and Public Health* [Preprint. https://doi.org/10.3390/ijerph15112494.
Nairn, J.R., Fawcett, R.J.B., 2014. The Excess Heat Factor: A Metric for Heatwave Intensity and its Use in Classifying Heatwave Severity. *International Journal of Environmental Research and Public Health* [Preprint. https://doi.org/10.3390/ijerph120100227.
Nogueira, P.J., 2005. Examples of heat health warning Systems: lisbon's ÍCARO's surveillance system, summer of 2003. In: Extreme Weather Events and Public Health Responses. https://doi.org/10.1007/3-540-28862-7_14.
Perkins, S.E., 2015. A Review on the Scientific Understanding of Heatwaves-Their Measurement, Driving Mechanisms, and Changes at the Global Scale. *Atmospheric Research* [Preprint. https://doi.org/10.1016/j.atmosres.2015.05.014.
Perkins, S.E., Alexander, L.V., 2013. On the measurement of heat waves. J. Clim. 26 (13), 4500–4517. https://doi.org/10.1175/JCLI-D-12-00383.1.
Perkins, S.E., Alexander, L.V., Nairn, J.R., 2012. Increasing Frequency, Intensity and Duration of Observed Global Heatwaves and Warm Spells. *Geophysical Research Letters*. https://doi.org/10.1029/2012GL053361.
Perkins-Kirkpatrick, S.E., Lewis, S.C., 2020. Increasing trends in regional heatwaves. Nat. Commun. https://doi.org/10.1038/s41467-020-16970-7.
Qiu, W., Yan, X., 2020. The trend of heatwave events in the Northern Hemisphere. Phys. Chem. Earth. https://doi.org/10.1016/j.pce.2020.102855 [Preprint].
Ranke, U., 2016. Natural Disaster Risk Management, Geosciences and Social Responsibility. Springer, Burgdorf, Germany. https://doi.org/10.1007/978-3-319-20675-2.

Royal Netherlands Meteorological Institute (KNMI), 2015a. European Climate Assessment & Dataset *[Online]*.
Royal Netherlands Meteorological Institute (KNMI), 2015b. European Climate Assessment & Dataset *[Online]*.
Royé, D., et al., 2020. Heat Wave Intensity and Daily Mortality in Four of the Largest Cities of Spain, vol. 182. Environmental research. https://doi.org/10.1016/J.ENVRES.2019.109027.
Russo, S., Sillmann, J., Fischer, E.M., 2015. Top Ten European Heatwaves since 1950 and Their Occurrence in the Coming Decades. *Environmental Research Letters* [Preprint. https://doi.org/10.1088/1748-9326/10/12/124003.
Scalley, B.D., et al., 2015. Responding to Heatwave Intensity: Excess Heat Factor Is a Superior Predictor of Health Service Utilisation and a Trigger for Heatwave Plans. *Australian and New Zealand Journal of Public Health* [Preprint. https://doi.org/10.1111/1753-6405.12421.
Schär, C., et al., 2004a. The Role of Increasing Temperature Variability in European Summer Heatwaves. *Nature* [Preprint. https://doi.org/10.1038/nature02300.
Schär, C., et al., 2004b. The Role of Increasing Temperature Variability in European Summer Heatwaves. *Nature* [Preprint. https://doi.org/10.1038/nature02300.
Schulzweida, U., Kornblueh, L., Quast, R., 2009. CDO User's Guide. Climate Data Operators. MPI for Meteorology. *Version 1.4.1*.
Sen, P.K., 1968. Estimates of the Regression Coefficient Based on Kendall's Tau. *Journal of the American Statistical Association* [Preprint. https://doi.org/10.1080/01621459.1968.10480934.
Smid, M., et al., 2019. Ranking European Capitals by Exposure to Heat Waves and Cold Waves. *Urban Climate* [Preprint. https://doi.org/10.1016/j.uclim.2018.12.010.
Sneyer, R., 1990. On the Statistical Analysis of Series of Observations. WMO Technical Note No. 143, Geneva, Switzerland.
Spinoni, J., Naumann, G., Vogt, J.V., 2017. Pan-European Seasonal Trends and Recent Changes of Drought Frequency and Severity. *Global and Planetary Change* [Preprint. https://doi.org/10.1016/j.gloplacha.2016.11.013.
Squintu, A.A., et al., 2020. Comparison of Homogenization Methods for Daily Temperature Series against an Observation-Based Benchmark Dataset. *Theoretical and Applied Climatology* [Preprint. https://doi.org/10.1007/s00704-019-03018-0.
Sunyer, J., 2010. Geographical differences on the mortality impact of heat waves in Europe. Environ. Health: A Glob. Access Sci. Source 9 (1), 1–2. https://doi.org/10.1186/1476-069X-9-38/PEER-REVIEW.
Thomas, K., et al., 2019. Explaining Differential Vulnerability to Climate Change: A Social Science Review. Wiley Interdisciplinary Reviews: Climate Change. https://doi.org/10.1002/wcc.565.
Tobias, A., et al., 2012. Mortality on Extreme Heat Days Using Official Thresholds in Spain: A Multi-City Time Series Analysis. *BMC Public Health* [Preprint. https://doi.org/10.1186/1471-2458-12-133.
Tolika, K., 2019. Assessing Heat Waves over Greece Using the Excess Heat Factor (EHF)," *Climate*. https://doi.org/10.3390/cli7010009 [Preprint].
Tomlinson, C.J., et al., 2011. Including the Urban Heat Island in Spatial Heat Health Risk Assessment Strategies: A Case Study for Birmingham, UK. *International Journal of Health Geographics* [Preprint. https://doi.org/10.1186/1476-072X-10-42.
UNDRO, 1979. Natural Disaster and Vulnerability Analysis. Office of the United Nations Disaster Relief Co-ordinator (UNDRO), Report of Expert Group. United Nations, Geneva, Switzerland.
United Nations, 2014. World Urbanization Prospects: 2014 Revision. https://doi.org/10.4054/DemRes.2005.12.9. New York, United.
Urban, A., et al., 2017. Impacts of the 2015 Heat Waves on Mortality in the Czech Republic-a Comparison with Previous Heat Waves. *International Journal of Environmental Research and Public Health* [Preprint. https://doi.org/10.3390/ijerph14121562.
Vandentorren, S., et al., 2006. Heat Wave in France: Risk Factors for Death of Elderly People Living at Home. European Journal of Public Health. https://doi.org/10.1093/eurpub/ckl063 [Preprint].
Vanderplanken, K., et al., 2021. Governing heatwaves in Europe: comparing health policy and practices to better understand roles, responsibilities and collaboration. Health Res. Pol. Syst. 19 (1), 1–14. https://doi.org/10.1186/S12961-020-00645-2/TABLES/3.
Williams, S., et al., 2012. Heat and Health in Adelaide, South Australia: Assessment of Heat Thresholds and Temperature Relationships. *Science of the Total Environment* [Preprint. https://doi.org/10.1016/j.scitotenv.2011.11.038.
Wolf, T., McGregor, G., 2013. The Development of a Heat Wave Vulnerability Index for London. *Weather and Climate Extremes* [Preprint, United Kingdom. https://doi.org/10.1016/j.wace.2013.07.004.
World Meteorological Organization, 2017. WMO Guidelines on the Calculation of Climate Normals. WMO-No. 1203. Geneva, Switzerland. Available at: https://library.wmo.int/doc_num.php?explnum_id=4166.
Xu, Z., et al., 2016. Impact of heatwave on mortality under different heatwave definitions: a systematic review and meta-analysis. Environ. Int. 89 (90), 193–203. https://doi.org/10.1016/J.ENVINT.2016.02.007.
Zare, S., et al., 2018. Comparing Universal Thermal Climate Index (UTCI) with selected thermal indices/environmental parameters during 12 months of the year. Weather Clim. Extrem. 19 https://doi.org/10.1016/j.wace.2018.01.004.
Zhang, Ruonan, et al., 2020. Increased European Heat Waves in Recent Decades in Response to Shrinking Arctic Sea Ice and Eurasian Snow Cover," *Npj Climate And Atmospheric Science*. https://doi.org/10.1038/s41612-020-0110-8 [Preprint].
Zhang, X., et al., 2011. Indices for Monitoring Changes in Extremes Based on Daily Temperature and Precipitation Data. *Wiley Interdisciplinary Reviews: Climate Change*. https://doi.org/10.1002/wcc.147.
Ziser, C.J., Dong, Z.Y., Saha, T.K., 2005. Investigation of weather dependency and load diversity on Queensland electricity demand. In: Australasian Universities Power Engineering Conference, 2005.